Geophys. J. R. astr. Soc. (1978) **55**, 615–632

Comparison of theoretical and observed temperature profiles in Devon Island ice cap, Canada

W. S. B. Paterson *Polar Continental Shelf Project, Department of Energy, Mines and Resources, Ottawa K1A 0E4, Canada*

G. K. C. Clarke *Department of Geophysics and Astronomy, University of British Columbia, Vancouver V6T 1W5, Canada*

Received 1978 April 25; in original form 1976 November 30

Summary. A non-steady-state theoretical model is used to predict the present variation of temperature with depth in two boreholes in the Devon Island ice cap, Arctic Canada. The boreholes are 300 m apart and one of them reaches bedrock. The heat transfer equation is solved numerically with the record of past temperatures obtained from measurements of the variations of oxygen–isotope ratio with depth in the cores as surface boundary condition. The effects of ice advection, refreezing of meltwater percolating from the surface (the amount of which is recorded in the cores), heating due to firn compaction and ice deformation, and heat flow in the bedrock below the ice sheet are all included in the model. The free parameters are geothermal heat flux, present surface temperature and heat loss at the surface which depends on the depth of meltwater penetration and other factors. Agreement between observed and predicted temperature–depth profiles is very close. Latent heat released by percolating meltwater is the predominating factor in determining the temperature distribution in the upper half of each borehole. The temperature distribution is insensitive to the value of the factor used to convert oxygen–isotope ratio to temperature.

1 Introduction

Modern study of the temperature distribution in polar ice sheets began with the analysis of Benfield (1951) of the effect of accumulation on temperatures in a snowfield and with the calculation by Robin (1955) of a steady-state temperature distribution in an ice sheet in which the effect of ice flow was taken into account. The first measured temperature profile through a polar ice sheet was obtained by Hansen & Langway from the borehole at Camp Century, Greenland (Weertman 1968). Weertman (1968), Dansgaard & Johnsen (1969) and Philberth & Federer (1971) have calculated theoretical profiles in reasonable agreement with the observations. All these are steady-state analyses with complicating factors that Robin (1955) did not consider. In fact, it is unlikely that any ice cap is ever in a steady state

for very long: thus a non-steady-state analysis seems preferable provided that sufficient input data are available. As a first step, Radok, Jenssen & Budd (1970) used an analysis in which it was assumed that temperature changed with time at a constant rate. They obtained satisfactory fits to the temperature distribution at Camp Century and also that at Byrd Station, Antarctica.

Over the past decade, cores recovered from polar ice sheets have provided a detailed record of climatic variations over periods of up to 125 000 yr (Epstein, Sharp & Gow 1970; Johnsen *et al.* 1972; Barkov *et al.* 1974; Paterson *et al.* 1977). Because the ratio of the concentrations of ^{18}O to ^{16}O in polar snow depends on its temperature of formation, variations of this ratio with depth in the ice can be interpreted as variations of temperature with time. The $^{18}O/^{16}O$ ratio is expressed as the fractional difference between the ratio in the sample to the ratio in 'standard mean ocean water'. It is denoted by δ and measured in parts per thousand (‰). The ratio is related to temperature because ^{18}O has a slightly lower vapour pressure than ^{16}O. Thus atmospheric water vapour will be depleted in ^{18}O relative to ocean water and, as an air mass moves to higher latitudes and higher elevations on an ice sheet, it will become progressively more depleted in ^{18}O, that is, δ will become more negative.

Confirmation of a relation between δ and the 'mean air temperature' is obtained by plotting these quantities for points on the Greenland and Antarctic Ice sheets (Dansgaard *et al.* 1973, figure 2). (On ice sheets the quantity measured is the temperature at 10 m depth; this may differ from the mean annual air temperature by 1 or 2 deg.) The 12 data points from the Greenland Ice Sheet are very well fitted by a relation

$$T = (\delta - \delta_0)/b + T_0 \qquad (1)$$

where T is temperature, δ_0 the surface value of δ, T_0 the corresponding temperature and b a constant with a value of $+0.62$‰ deg^{-1}. A straight-line relationship also holds for Greenland coastal stations. However, the values of T_0 and b differ from the ice sheet values. Data from the Antarctic Ice Sheet show the same trend but more scatter. Because of this relationship between δ and T at different places, the assumption is made that a similar relationship holds at one place at different times. Thus a profile of δ versus depth can be interpreted as a relationship between temperature and time and this can then be used as the surface boundary condition in non-steady-state solutions of the heat transfer equation. However, the only published analysis of this kind is that of Johnsen (1977) using data from a 50-m borehole at Crête in central Greenland.

In this paper we describe the method and results of such an analysis of data from two boreholes, one of which reaches bedrock, in the Devon Island ice cap, in Arctic Canada. The fact that the ice is only 300 m thick, compared with one or two thousand metres in Greenland and Antarctica limits the analysis in certain respects. On the other hand, more glaciological information is available for the Devon Island ice cap than is the case at Camp Century and Byrd Station and we wanted to devise a model making full use of this information. Our model includes the heating effect of the refreezing of percolating surface meltwater; this is significant at Devon Island though probably not at Camp Century and certainly not at Byrd Station.

2 Field measurements

Fig. 1 shows Devon Island ice cap and its location. The ice cap lies in the eastern part of the island, has an area of about 15 600 km^2 and a maximum elevation of about 1900 m. Measured ice thicknesses range from 200 to 1000 m. The ice cap has an east–west summit ridge. The boreholes used in this study, Holes 71 and 72, are about 600 and 900 m north of

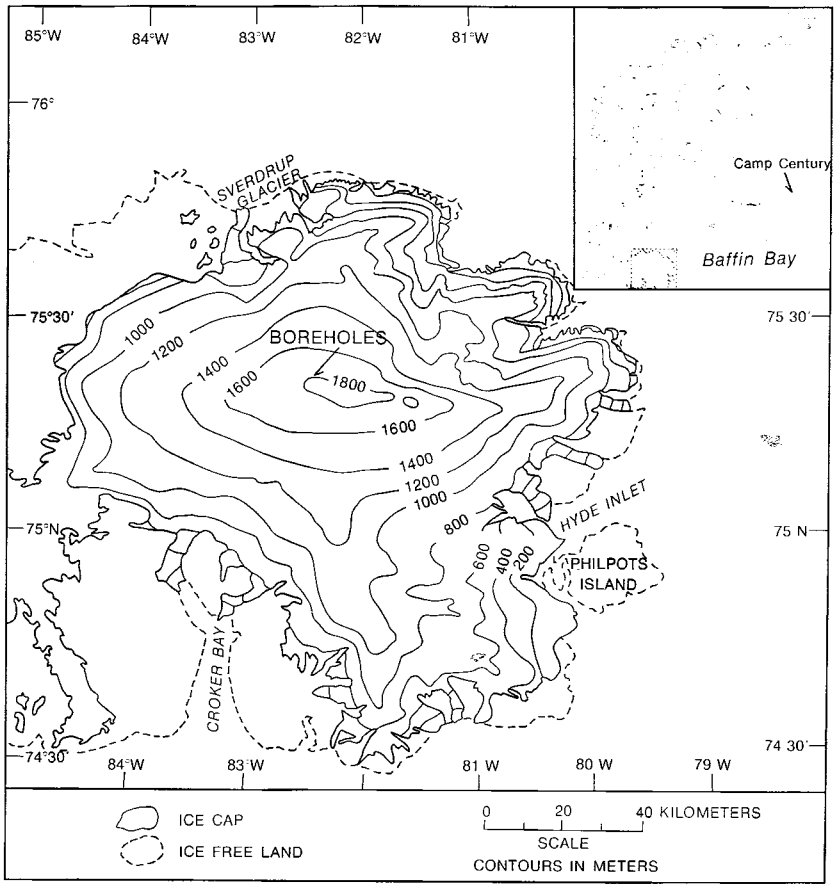

Figure 1. Map of the Devon Island ice cap.

the ridge crest and about 7.5 km west of its highest point. The surface elevation at Hole 72 is about 1825 m and the surface slope 1.5°. Hole 72 reached bedrock at a depth of 299 m; Hole 71 is 220 m deep and the ice thickness is about 300 m. Annual precipitation is 0.22 m, water equivalent. Some melting occurs in most summers. The meltwater percolates into the snow and refreezes to form ice layers and lenses.

2.1 BOREHOLE TEMPERATURES

Temperature was measured with two thermistors at intervals varying from 2 to 5 m throughout both boreholes. Measurements were made 1 yr after drilling to ensure that perturbations introduced by the drilling had died out. The thermistor calibration was good to 0.01 deg. This is also the rms difference between the readings of the two thermistors and so is taken as the standard error of each temperature.

2.2 ICE VELOCITY

The component of velocity parallel to the surface (u) was determined as a function of depth y in Hole 72 by measuring the change in tilt of the borehole over a 4-yr period (Paterson, unpublished data). This gives $\partial u/\partial y$. Velocity was obtained by numerical integration on the

assumption of zero velocity at the bed. This is reasonable because the measured basal temperature of $-18.4°C$ shows that the ice is frozen to its bed. The component of velocity normal to the surface (v) was determined as a function of y by measuring the change in length of sections of borehole over 1 yr (Paterson 1976). No horizontal velocity measurements were made in Hole 71, so the Hole 72 values were taken. These velocities are used in calculating the strain heating. As this turns out to be negligible, use of the Hole 72 values at Hole 71 will not introduce any significant errors. An incomplete set of measurements of v in Hole 71 suggested that the values did not differ from those in Hole 72. The Hole 72 values were therefore used in both holes.

2.3 DENSITY

Density was measured in Hole 72 by weighing the core in 1.5-m sections and calculating volume from its dimensions. This is the most satisfactory method of obtaining mean densities when the core is inhomogeneous due to the presence of ice layers among the compacted snow. Density was 388 kg m^{-3} at the surface. The density of 820 kg m^{-3}, at which point the entrapped air is sealed into the form of bubbles and the material is considered to change from 'firn' to ice, was reached at a depth of 60 m. There was no measurable density change below 95 m. The density versus depth curve was smoothed before being used for calculations of thermal conductivity. The values for Hole 72 were also used for Hole 71 because densities were not measured there. Ice layers and lenses will probably differ in thickness and position between the two holes and this will result in minor differences in detail between their depth–density curves. However, as the holes are only 300 m apart, systematic differences between their depth–density curves were not expected.

2.4 TIME-SCALE

The age t of the ice at depth y (measured normal to the surface) in both boreholes was determined by the formula

$$t = \int_0^y [1/v(y')]\, dy' \qquad (2)$$

using numerical integration of values of v measured in Hole 72. These ages were checked by measurements of the thickness of annual layers of ice based on variations in microparticle concentration and by absolute dating of the ice by the ^{32}Si and ^{14}C methods. The last 5250 yr of core are believed to be well dated. Dates in the period 5250 to 11 000 BP are subject to some uncertainty and there may be short gaps in this part of the record. Beyond 11 000 BP the dating is unreliable (Paterson *et al.* 1977).

2.5 OXYGEN ISOTOPE RATIOS

The oxygen isotope ratio δ was measured throughout the core from Hole 72 and also from another hole, Hole 73, 27 m away. No isotope ratios were measured in Hole 71. Down to a depth of about 100 m, which corresponds to the last 500 yr of record, the length of each sample was equal to the mean thickness of one annual layer. For the period 500 to 10 000 BP, the sample length was the mean thickness of five annual layers. In the lowest 5 m of core, which spans the period 10 000 to about 125 000 BP, the sample length was 10 mm. Because the effect of surface temperature variations with periods of one or a few years is rapidly attenuated with depth, time averages of δ were used as surface boundary

condition in the present study. Five-year averages were used for the period 0–500 BP and 50-yr averages before that. Any small gaps in the record probably have a negligible effect on the 50-yr means. For the present study the record was terminated at 11 000 BP because the dating is unreliable beyond this point. Because the large rapid temperature increase that marked the end of the Wisconsin glaciation occurred at about 10 000 BP, its effect is included in the analysis. Comparison of values of δ measured in Holes 72 and 73 indicates that the standard error of a 50-yr mean δ is about 0.14‰ corresponding to a temperature error of about 0.25 deg (Paterson *et al.* 1977). The mean values of δ from Holes 72 and 73 were used as surface boundary condition in the analysis for both Holes 71 and 72.

2.6 MELTWATER CONTENT

Under present climatic conditions at the borehole sites, some snow melts in about nine summers out of 10. This water percolates into the snow and refreezes to form distinct stratigraphic features that can be identified down to a depth of about 150 m which corresponds to an age of about 800 yr. Koerner (1977) has studied the distribution and thickness of these features as a function of depth in each borehole. The density of the core is also known as a function of depth. Thus the variation of 'meltwater content' (the percentage, by weight, of core formed by refreezing of meltwater) with depth can be determined. From this, the latent heat generated by this process can be calculated as a function of time. The depth interval over which average water content was determined corresponds to time intervals between 4 and 15 yr. Cores from the upper 10 or so metres were of poor quality and could not be analysed; below a depth corresponding to about 800 BP, microfractures produced by the drilling obscured the stratigraphy.

The melt record for Hole 71 spans the period 17–727 BP and that for Hole 72 the period 47–812 BP. The average melt computed for the period 47–727 BP for which data from both holes are available is 6.38 per cent for Hole 71 and 6.16 per cent for Hole 72 giving a combined average of 6.27 per cent. The melt data for Hole 71 were used to replace the missing data from 17–47 BP for Hole 72; likewise data from Hole 72 were used to extend the record from Hole 71 from 727–812 BP. A constant melt of 15 per cent, obtained from surface pit data (Koerner 1977), was used to fill the 0–17 BP gap in both records. Lastly, the data had to be extrapolated back in time, beyond the 812 yr covered by measurements. From 812 BP to the end of the Wisconsin Glaciation at 10 000 BP, the mean value for both boreholes was used. From 10 000 to 11 000 BP, the starting point of the analysis, the meltwater was taken to be zero. Note that, in the analysis for each hole, we used the melt content record measured in that hole. However, we had to use the same isotope record in both holes because isotope ratios were not measured in Hole 71. We feel that this is reasonable since the two sites were probably subjected to the same climatic variations, although their response (i.e. surface melt) to these variations appears to have differed.

3 Heat transfer in ice sheets

The equation for conservation of energy in a deforming continuum can be written

$$\rho\left(\frac{\partial e}{\partial t} + v_m \frac{\partial e}{\partial x_m}\right) = f - \frac{\partial q_m}{\partial x_m} \tag{3}$$

(*cf.* Prager 1961, p. 87; Fung 1965, p. 346) where e is the specific internal energy, x_m the position vector, v_m the velocity vector, f is the rate of internal heat production per unit volume and q_m is the heat flux vector. The assumptions leading to equation (3) are that no rotational stresses or body forces are present. In (3) and throughout this paper the

summation convention is assumed. For ice sheets f is the sum of the strain heating and latent heat contributions so that

$$f = \sigma_{ij}\dot{\epsilon}_{ij} + Jw \tag{4}$$

where σ_{ij} is the stress tensor, $\dot{\epsilon}_{ij}$ the strain rate tensor, J the mechanical equivalent of heat (equal to unity in SI units) and w is the rate of release of heat per unit volume due to freezing of meltwater. The heat flux by thermal conduction can be written

$$q_m = -JK\partial T/\partial x_m \tag{5}$$

where K is the thermal conductivity.

For ice sheets all internal energy is in the form of thermal energy so that

$$e = J\int_0^T c(T')dT' \tag{6}$$

where c is the specific heat at constant volume. Substitution of (5) and (6) into (3) gives the general equation for heat transfer in ice sheets

$$\rho cJ\left(\frac{\partial T}{\partial t} + v_m\frac{\partial T}{\partial x_m}\right) = f + J\frac{\partial K}{\partial x_m}\frac{\partial T}{\partial x_m} + JK\nabla^2 T \tag{7}$$

or

$$\frac{1}{\kappa}\left(\frac{\partial T}{\partial t} + v_m\frac{\partial T}{\partial x_m}\right) = \frac{f}{KJ} + \frac{1}{K}\frac{\partial K}{\partial x_m}\frac{\partial T}{\partial x_m} + \nabla^2 T \tag{8}$$

where $\kappa = K/\rho c$ is the thermal diffusivity.

4 The model

The main assumptions we used to simplify (8) and to construct our heat transfer model are as follows:

(a) The ice thickness in the vicinity of the borehole site has remained constant over the past 11 000 yr and during that period there has been no time variation in the density, thermal properties or velocity field. This assumption appears to be very sound over the past 3200 yr; its validity over the longer period is less certain (Paterson *et al.* 1977).

(b) Heat conduction normal to the surface of the ice sheet is the only significant component of heat conduction. We locate the origin of coordinates at the surface of the ice sheet and take y as the depth variable with y directed positive downward; the x axis is aligned parallel to the flow direction; thus our assumption is that $\partial^2 T/\partial x^2 = \partial^2 T/\partial z^2 = 0$. Measurements of 10-m temperatures in the vicinity of the borehole show that these derivatives are indeed extremely small.

(c) The only significant component of advective heat transfer is that normal to the surface. The advective terms $u\partial T/\partial x$ and $w\partial T/\partial z$ are negligible because near an ice divide the flow components u and w, as well as the temperature gradients $\partial T/\partial x$ and $\partial T/\partial z$, are small.

With the above assumptions the heat transfer equation in the ice sheet simplifies to

$$\frac{\partial^2 T}{\partial y^2} + \left(\frac{1}{K}\frac{dK}{dy} - \frac{v}{\kappa}\right)\frac{\partial T}{\partial y} - \frac{1}{\kappa}\frac{\partial T}{\partial t} = \frac{-f}{KJ}. \tag{9}$$

The variation of thermal conductivity with depth is not a measured quantity so we make the further assumption:

(d) The thermal conductivity variation in the firn layer can be adequately approximated by a law relating conductivity to firn density. In this way the term dK/dy in (9) can be replaced by $dK/dy = (dK/d\rho)\,(d\rho/dy)$ where $d\rho/dy$ is calculated from the measured density variation with depth and $dK/d\rho$ is given by an empirical or theoretical conductivity law. Thermal diffusivity was calculated by the relation $\kappa(y) = K[\rho(y)]/\rho(y)c$.

In order to obtain an estimate of the effect of surface melting on the temperature profile we assume:

(e) That the meltwater content deduced from the core can be used to calculate the latent heat injection due to surface melt.

Because the large temperature change at the end of the Wisconsin glaciation affects the temperature gradient at the base of the ice, we also consider heat transfer in the underlying bedrock.

(f) The heat transfer equation in the bed is

$$\frac{\partial^2 T}{\partial y^2} - \frac{1}{\kappa_b}\frac{\partial T}{\partial t} = 0 \qquad (10)$$

where κ_b is the thermal diffusivity of the bed (assumed constant).

Lastly we assume boundary and initial conditions:

(g) The surface temperature boundary condition of the ice cap is given by the measured δ variations through equation (1).

(h) Heat flux $-K\partial T/\partial y$ is continuous across the ice–rock interface.

(i) The basal boundary condition is that at some depth below the ice sheet the upward heat flux G is constant with time. As no geothermal flux measurements have been made on Devon Island, this constant may be varied to fit the observations.

(j) The initial temperature (11 000 BP) is assumed to increase linearly with depth and to satisfy the boundary conditions; temperature gradient is derived from the assumed geothermal flux, and surface temperature from the δ value for 11 000 BP. Because the present temperature profile is not sensitive to the choice of initial conditions, there is little point in assuming anything more complicated than a linear profile.

5 Derived data

5.1 SURFACE TEMPERATURE

The surface temperature boundary condition is calculated directly from the record of δ variations with time. The time interval between successive δ values varies from 5 to 50 yr; to obtain a continuous function, linear interpolation between observations is used, thus

$$T_s(t) = [\delta(t) - \delta_0]/b + T_0 \qquad (11)$$

where T_s is surface temperature, $\delta(t)$ the δ value at time t, $\delta_0 = -27.60$‰ deg^{-1} the present value near the surface at the boreholes and T_0 is the temperature corresponding to δ_0. In the dry snow zone of cold ice masses where no surface melting occurs, T_0 would approximate the 10-m temperature in the firn and could easily be measured. Owing to percolation of summer melt into the firn we believe that the 10-m temperature is warmer than the mean

surface temperature. We therefore leave T_0 as a free parameter to be determined by fitting the calculated temperature profile to the measured one. Because the surface at Hole 71 is 6 m higher than at Hole 72, temperatures in Hole 71 should be systematically colder by about 0.05 deg. This is in fact the case, but we neglect this small difference and assume the surface temperature is the same in both holes.

To choose a value for b, we used the observation of Koerner (private communication) that δ decreases by 0.589‰ per 100 m increase of elevation on the south-east side of the Devon Island ice cap. (The main source of precipitation is to the south-east.) This has to be combined with a lapse rate to determine b. The appropriate lapse rate for precipitation conditions is the wet adiabatic lapse rate of 0.6 deg per 100 m. This gives the value $b = 0.98$‰ deg^{-1} that we used. We shall show later, however, that the predicted temperature distribution is insensitive to the value of b.

5.2 LATENT HEAT RELEASE

Stratigraphic features in the core provide a record of surface melting over the past 800 yr, as described previously. From these measurements we construct the time series $P(t)$, the variation with time of measured percentage meltwater content (water equivalent). A continuous reconstruction of $P(t)$ between measurements is obtained by linear interpolation so that $P(t)$ has a saw-toothed appearance. Because $P(t)$ is measured at irregular times and is not a smoothly varying function of time, we replace $P(t)$ in our calculations by its time average

$$\langle P(t)\rangle = \frac{1}{2\Delta t}\int_{t-\Delta t}^{t+\Delta t} P(t')dt' \tag{12}$$

where Δt is the time step of the finite-difference scheme (*cf.* Appendix). The average rate of release of thermal energy due to refreezing of surface melt is

$$W_0(t) = Lv_0\rho_0 P(t)/100 \tag{13}$$

where v_0 is the downward velocity at the surface of the ice sheet, ρ_0 is the density of the near-surface layer, and $L = 3.35 \times 10^5$ J/kg is the latent heat of fusion of water. Equation (13) will, in fact, underestimate the heating effect because only part of the refrozen meltwater forms distinct features that can be recognized in the core. Koerner (private communication) has studied this by measuring the density change during the summer in the near-surface layers and assuming that all the density change resulted from melting. In three years of data the percentage of the total melt observed in a core varied from 33–78 per cent. Because of this wide variation we regard the 'melt factor' M (the number by which the meltwater content observed in the core has been multiplied to give the total melt) as an adjustable parameter in the analysis. We therefore modify (13) to

$$W_0(t) = Lv_0\rho_0 MP(t)/100. \tag{14}$$

Lastly we assumed that the latent heat was not released at a single discrete depth but rather was distributed over a narrow near-surface zone. The spatial distribution for latent heat release was taken as

$$g(y) = \frac{2}{l_0^2}\{l_0 - 2|y-d|\} \qquad d - \frac{l_0}{2} \leqslant y \leqslant d + \frac{l_0}{2}$$
$$= 0 \qquad |y-d| > l_0/2 \tag{15}$$

where l_0 is the width and d the depth to the middle of the wetted zone. The function $g(y)$ has a triangular shape and is normalized so that its integral over y is unity. We do not expect our results to be very sensitive to the shape of $g(y)$, but it is necessary to assume some particular shape before calculations can proceed. In reality, the parameters l_0 and d vary greatly from year to year and so are ill-determined; we therefore take them as free parameters in our model. In addition to the latent heat contribution, thermal energy is released as the newly-frozen ice cools to the ambient temperature of the surrounding ice. Thus the average rate of release of heat due to the presence of meltwater at depth y and time t is

$$w(y, t) = [1 + c(T_m - T)/L]Lv_0\rho_0 Mg(y)\langle P(t)\rangle/100 \tag{16}$$

where T_m is the melting temperature.

5.3 CONDUCTIVITY

In the upper 90 m of Devon Island ice cap at Hole 72 the density varies from 387.8 to 905.0 kg m^{-3} and a wide variation in thermal conductivity is to be expected. Numerous empirical and theoretical formulae have been proposed to express the variation of thermal properties of firn with density. Unfortunately a number of factors besides density influence the thermal properties of firn so there is a wide scatter between the various formulae. A common starting point is that the specific heat is taken to be independent of density and equal to that for ice, namely $c = 2009.06$ J kg^{-1} deg^{-1}. We use the Van Dusen Formula cited in Bader & Kuroiwa (1962)

$$K(\rho) = 0.021 + 0.00042\rho + 2.2 \times 10^{-9}\rho^3 \tag{17}$$

with K in W m^{-1} deg^{-1} and ρ in kg m^{-3}.

5.4 STRAIN HEATING

The rate of heat production per unit volume due to strain heating is

$$\sigma_{ij}\dot{\epsilon}_{ij} = \sigma_{xx}\dot{\epsilon}_{xx} + \sigma_{yy}\dot{\epsilon}_{yy} + \sigma_{zz}\dot{\epsilon}_{zz} + 2(\sigma_{xy}\dot{\epsilon}_{xy} + \sigma_{xz}\dot{\epsilon}_{xz} + \sigma_{yz}\dot{\epsilon}_{yz}). \tag{18}$$

From the measured values of $u(y)$ and $v(y)$, the strain rate components $\dot{\epsilon}_{xy}(y)$ and $\dot{\epsilon}_{yy}(y)$ can be computed by numerical differentiation. Near the boreholes $\dot{\epsilon}_{zz}$ at the surface is an order of magnitude less than $\dot{\epsilon}_{xx}$; we assume this remains true at depth so that the flow is two-dimensional giving $\dot{\epsilon}_{zz} = \dot{\epsilon}_{yz} = \dot{\epsilon}_{xz} = 0$. Strain heating in the firn layer is primarily due to compaction while in the ice, which is incompressible, creep flow is the source of heat generation. Our treatment of these two processes differs so we discuss them separately.

5.4.1 Firn compaction

The principle of conservation of mass gives the continuity equation

$$\frac{\partial\rho}{\partial t} + v_i\frac{\partial\rho}{\partial x_i} = -\rho\dot{\epsilon}_{ii}. \tag{19}$$

Our previous assumption $\partial\rho/\partial t = 0$ (Sorge's Law) and the plausible assumption that macroscopic lateral density gradients are negligibly small gives

$$\dot{\epsilon}_{xx} + \dot{\epsilon}_{yy} + \dot{\epsilon}_{zz} = \frac{-v}{\rho}\frac{d\rho}{dy}. \tag{20}$$

In the firn the stress components σ_{xx}, σ_{yy} and σ_{zz} are primarily hydrostatic so that

$$\sigma_{xx} = \sigma_{yy} = \sigma_{zz} = -\frac{1}{3}p \tag{21}$$

where

$$p = g\int_0^y \rho(y')dy' \tag{22}$$

and thus

$$\sigma_{xx}\dot{\epsilon}_{xx} + \sigma_{yy}\dot{\epsilon}_{yy} + \sigma_{zz}\dot{\epsilon}_{zz} = \frac{pv}{3\rho}\frac{d\rho}{dy} \quad . \tag{23}$$

Addition of the term due to the non-vanishing shear stress component

$$\sigma_{xy} = g \sin\alpha\int_0^y \rho(y')dy' \tag{24}$$

gives the complete strain heating contribution

$$\sigma_{ij}\dot{\epsilon}_{ij} = \frac{pv}{3\rho}\frac{d\rho}{dy} + 2\sigma_{xy}\dot{\epsilon}_{xy}. \tag{25}$$

5.4.2 *Creep deformation of ice*

Glacier ice is incompressible so that

$$\dot{\epsilon}_{xx} + \dot{\epsilon}_{yy} + \dot{\epsilon}_{zz} = 0 \tag{26}$$

because $\dot{\epsilon}_{zz} = 0$ and $\dot{\epsilon}_{xx} = -\dot{\epsilon}_{yy}$ for two-dimensional flow, the second invariant of the strain rate tensor can be written

$$E_2 = \dot{\epsilon}_{yy}^2 + \dot{\epsilon}_{xy}^2. \tag{27}$$

The generalized flow law for ice (Glen 1958) relates components of the deviatoric stress tensor to strain rate components and allows evaluation of the strain heating term in f. The flow law is

$$\dot{\epsilon}_{ij} = B_0 \exp(-Q/RT)\ (\Sigma_2')^{(n-1)/2}\sigma_{ij}' \tag{28}$$

where B_0 is a constant, Q is the activation energy for creep, R the gas constant, n the flow law exponent, σ_{ij}' the deviatoric stress tensor and $\Sigma_2' = \frac{1}{2}\sigma_{ij}'\sigma_{ij}'$ its second invariant. The rate of heat generation by strain heating is therefore

$$\sigma_{ij}\dot{\epsilon}_{ij} = 2[B_0 \exp(-Q/RT)]^{-1/n}E_2^{(n+1)/2n} \tag{29}$$

the constants n, B_0 and Q have been experimentally determined and we take $n = 3$, $B_0 = 0.875 \times 10^{-12}\,\mathrm{N^{-3}\,m^6\,s^{-1}}$ and $Q = 6.07 \times 10^4\,\mathrm{J\ mole^{-1}}$ to obtain a flow law lying in the middle range of flow laws quoted by Weertman (1973).

No measurable density change occurs below 95 m; we therefore take this as the depth at which one passes from strain heating by firn compaction to strain heating by creep deformation of ice. This choice is arguable but in the present case the effect of strain heating on the calculated temperature profiles is barely noticeable so the question is of little importance.

6 Modelling results

Although such quantities as the ice flow law parameters and thermal properties of the bed appear in our physical description, their influence on our results is small and uninteresting. The key variables of our model are the following:

(a) present surface temperature, T_0,
(b) geothermal flux, G,
(c) depth to the centre of the wetted zone, d,
(d) width of the wetted zone, l_0,
(e) multiplying factor to transform measured melt to total melt, M,

though we, in fact, will discover that only three variables significantly influence the calculated temperature profile.

By numerical testing it was discovered that the width of the wetted zone has an imperceptible effect on the calculated temperatures; on the other hand, the depth, d, to the centre of the wetted zone is extremely influential. This sensitivity is not surprising because varying d is equivalent to varying the efficiency of trapping of latent heat in the ice sheet: if d is large most of the thermal energy due to melting is stored in the ice sheet, if d is small most escapes by conduction at the surface. Our model takes no account of seasonal variations in surface conditions and assumes that thermal conduction is the only means of heat transfer at the surface. This is a gross oversimplification: a rigorous treatment would introduce additional parameters describing heat transfer at the snow–air interface; their combined effect is represented by our single parameter d. The choice of melt factor M also has an important effect on the calculated temperatures because the larger M, the more latent heat is supplied to the firn. The parameters d and M are interrelated, however, in that a change in one can always be compensated by changing the other. Observations at Hole 72 suggest that the true wetted depth seldom exceeds 1 m (Koerner, private communication). We therefore choose $d = 1.0$ m and adjust the value of M to give a good fit to the data. The best value is 2.5 which implies that, on average, less than half the total melt is observed in the core. This was the case in two of the three years for which observations were made (Koerner, private communication); with this value total melt never exceeded 100 per cent. Use of a different law relating conductivity to density would give a different conductivity in the upper layers; this would also change the surface heat loss which could again be compensated by choosing a different value of M. Thus in reality there are only three free parameters in our model:

(a) surface temperature, T_0,
(b) geothermal flux, G,
(c) surface heat flux (controlled by the choice of d, M and conductivity law).

Fig. 2(a) and (b) show computed and measured temperature profiles in the two boreholes; Fig. 3 shows the details of the fit in the uppermost 120 m of both holes. Table 1 lists the model parameters (Model A). The curves fit the data very well; the maximum deviation between calculated and measured temperatures is 0.04 deg. The only difference between the models for the two holes is in the amount of meltwater and this difference convincingly explains the difference between the observed temperatures in the top 120 m of the two holes. This suggests that latent heat released by refreezing meltwater is the major factor in determining the temperature distribution in the upper parts of these boreholes. It also suggests that out very simple model of heat transfer in the near-surface layers is adequate for explaining the observations. The misfit in the uppermost 20 m is to be expected since, as discussed previously, for Hole 71 the melt record from 0–17 BP is missing and for Hole 72

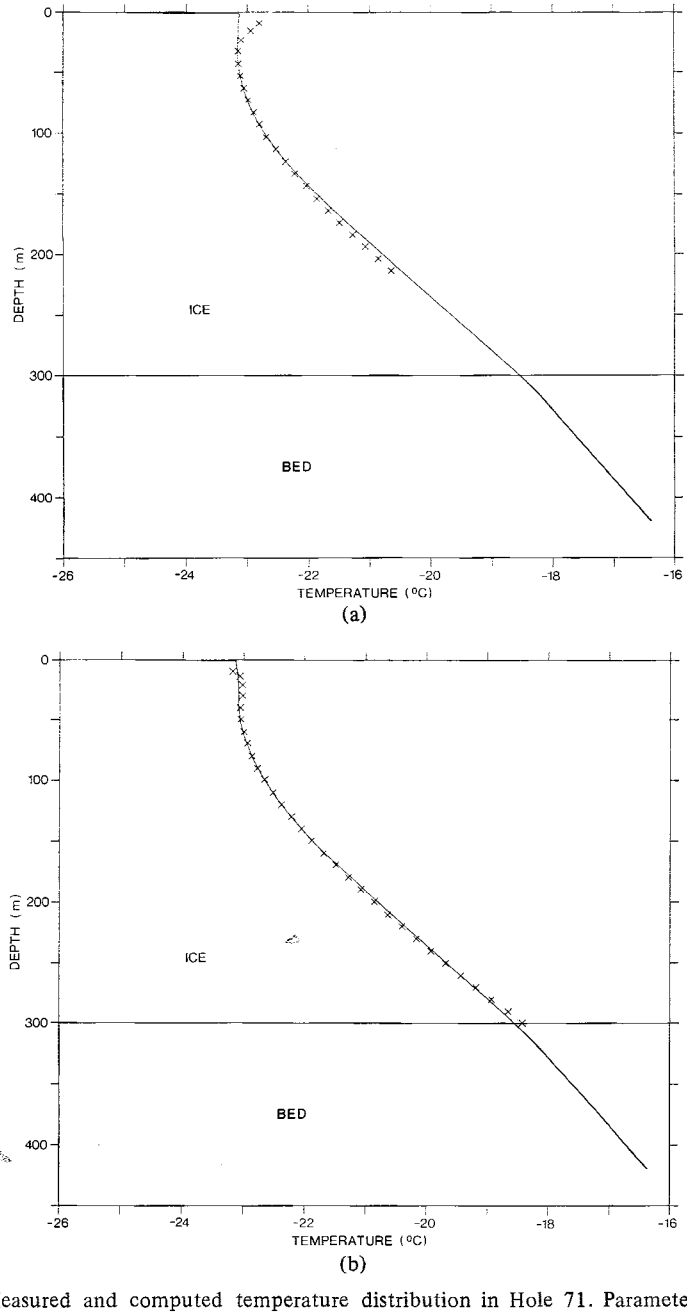

Figure 2. (a) Measured and computed temperature distribution in Hole 71. Parameters are those for Model A in Table 1. For clarity, only every second measurement is shown. (b) Measured and computed temperature distribution in Hole 72. Parameters are those for Model A in Table 1. For clarity, only every second measurement is shown.

the record from 0–47 BP is missing. Fig. 4 provides further evidence of the importance of meltwater in determining the temperature distribution. The curve represents the best fit to the observed temperatures in the lowest 150 m of Hole 72 when the meltwater input is set to zero. The parameters are given in Table 1 (Model B). Discrepancies between

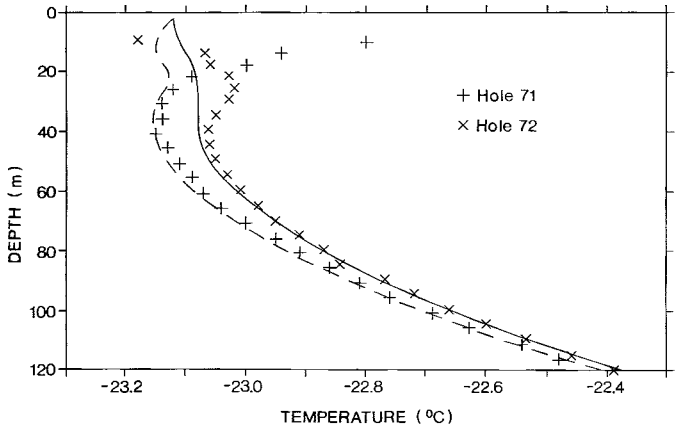

Figure 3. Details of observed and predicted temperatures in the uppermost 120 m of Holes 71 and 72. The dashed curve represents the fit to Hole 71.

Table 1. Devon Island ice cap models.

Model parameters	Model A	Model B	Model C	
Ice sheet thickness, h	299	299	299	m
Geothermal flux, G	0.043	0.045	0.050	W m^{-2}
	1.028	1.076	1.195	HFU
Present surface temperature, T_0	−25.8	−24.6	−24.9	°C
Present surface δ_0 value	−27.60	−27.60	−27.60	‰
Conversion factor, b	+ 0.98	+ 0.98	+ 0.98	‰ deg^{-1}
Bed conductivity, K_b	2.50	2.50	2.50	W m^{-1} deg^{-1}
Bed diffusivity, κ_b	1.37×10^{-6}	1.37×10^{-6}	1.37×10^{-6}	m^2 s^{-1}
Percolation depth, d	1.0	–	–	m
Width of wetted zone, l_0	0.20	–	–	m
Melt factor, M	2.5	–	–	
Ice conductivity, K	2.032	2.032	2.032	W m^{-1} deg^{-1}
Ice diffusivity, κ	1.12×10^{-6}	1.12×10^{-6}	1.12×10^{-6}	m^2 s^{-1}

theoretical and observed temperatures reach 1.5 deg; no model in which meltwater is neglected can reproduce the isothermal layer in the uppermost 60 m. The model suggests that the latent heat raises the 10-m temperature about 2.8 deg above the surface temperature.

Fig. 5 shows the effect of varying the parameter d, the meltwater penetration depth. All the other parameters have the same value as Model A in Table 1. The value chosen for d has a major effect on the temperature distribution because it determines how much of the latent heat is available to heat the firn and how much is lost by conduction to the surface. In fact, the penetration depth varies significantly from year to year and in about one year in 10 there is no melting at all. However, the value of 1 m chosen to give a best fit to the measured temperatures is a reasonable average (Koerner, private communication).

Fig. 6 shows the effect on the predicted temperature distribution of varying the value of b, the reciprocal of the regression coefficient of temperature on oxygen isotope ratio (equation (1)). All other parameters had the same values as in Model A (Table 1). For the dashed line, b was chosen as 2.00; with this value the observed difference in oxygen isotope ratios at 11 000 BP and present corresponds to a temperature difference of 4 deg. This is

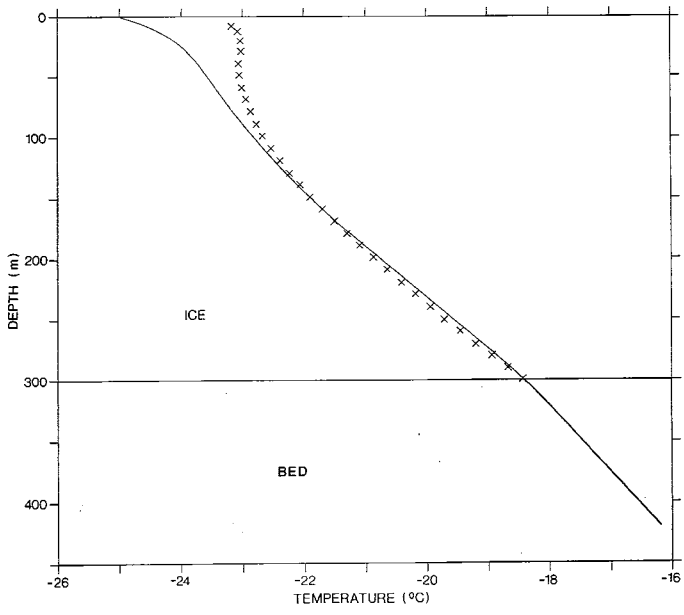

Figure 4. Measured temperature distribution in Hole 72 and the theoretical curve that gives the best fit to the lowest 150 m when the effect of meltwater is ignored (Model B in Table 1).

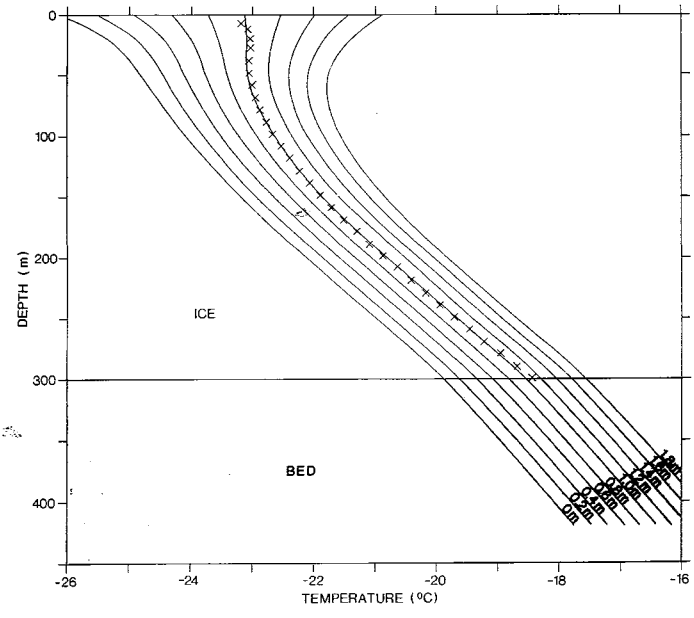

Figure 5. Measured temperature distribution in Hole 72 and theoretical curves for different values of melt penetration depth with all other parameters as for Model A (Table 1).

almost certainly too small. The value of b chosen for the solid line, namely 0.50, gives a temperature difference of 16 deg which is unreasonably high. Varying b over this very large range changes the predicted temperature distribution by a maximum of only 0.25 deg. To determine the value of b in any particular region is important because only if b is known can

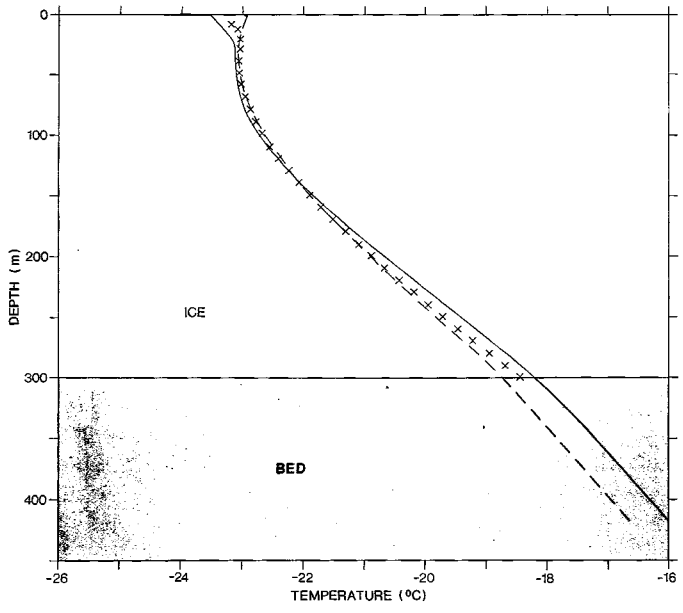

Figure 6. Measured temperature distribution in Hole 72 and theoretical curves for different values of the reciprocal b of the regression of temperature on oxygen isotope value. Dashed curve is for $b = 2.00$; solid curve for $b = 0.50$.

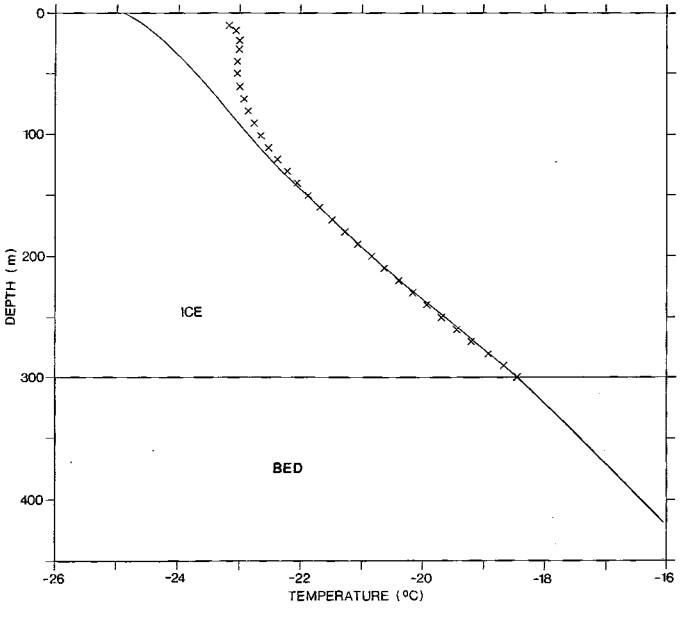

Figure 7. Measured temperature distribution in Hole 72 and steady-state distribution that gives the best fit to the lowest 150 m (Model C in Table 1).

δ values be transformed into temperatures. However, this test shows that the Devon Island boreholes are unsuitable for testing the applicability of any particular value of b. This is because variations in the latent heat released by refreezing of meltwater are much more important than variations in surface temperature in determining the temperature

distribution. Such a test should be made at a place where melting is negligible. In addition, a borehole considerably deeper than 300 m is desirable. Temperatures in the lower half of the Devon boreholes are determined largely by the geothermal heat flux. In a thicker ice cap, the surface temperature is the major factor in determining temperature to a much greater depth than is the case here.

Although the geothermal flux used in the model is an acceptable value for the Devon Island region, it should not be interpreted as the true geothermal flux. The chosen value depends on the thickness of the rock layer in the model (in our case 120 m). The estimate cannot be improved by increasing the thickness of this layer because the effect of the assumed initial conditions would then become increasingly important.

Steady-state models are often used to predict temperature distributions in ice caps. Fig. 7 shows the best-fitting steady-state temperature distribution for the lowest 150 m of Hole 72. The parameters are given in Table 1 (Model C). In these calculations the meltwater merely introduces a displacement between the surface temperature and the temperature in the zone immediately below the melt penetration depth. We therefore take the melt percentage as zero with the understanding that the surface temperature in Fig. 7 must be interpreted as the firn temperature immediately below the zone of melt penetration. Although this curve fits the observations in the lowest 150 m very well, no steady-state model gives a curve of the shape observed in the upper part of the boreholes and discrepancies between predictions and observations range up to 1.5 deg. The inflection in the theoretical curve near a depth of 50 m results from the rapid change in thermal properties of the firn layer with depth.

7 Conclusions

Our model gives a predicted distribution of ice temperature with depth that agrees closely with that observed in a borehole through the ice cap. It also successfully predicts the small differences between temperatures observed in the upper parts of two boreholes 300 m apart. The analysis shows that variations in the latent heat produced by refreezing of percolating meltwater are much more important than surface temperature variations in determining the temperature distribution. The model provides a means of estimating the amount of latent heat. Although a value has to be chosen for the regression coefficient of temperature on oxygen isotope ratio, the analysis shows that, in this instance, the predicted temperature distribution is insensitive to the particular value chosen. Strain heat is also included although its effect turns out to be negligible.

To apply the model, the following quantities must be measured as functions of depth: density, oxygen isotope ratio, meltwater content, velocity components parallel and normal to the surface and the age of the ice. Age can be calculated from the measured normal velocity but it should be checked by measurements of annual layer thickness based on seasonal variations in oxygen isotope ratio or in microparticle concentration, or by absolute dating by the ^{32}Si and ^{14}C methods. All these data are available for the borehole site on Devon Island; this is not the case in Greenland and Antarctica. The model could be further refined if thermal conductivity were measured as a function of depth.

Acknowledgments

WSBP thanks the Department of Geophysics and Astronomy at the University of British Columbia for hospitality and donation of computer time. We thank R. M. Koerner for helpful discussion and access to unpublished data. G. de Q. Robin's valuable criticism is

gratefully acknowledged. The National Research Council of Canada, Environment Canada and the University of British Columbia Committee on Arctic and Alpine Research provided financial support.

References

Bader, H. & Kuroiwa, D., 1962. The physics and mechanics of snow as a material, *Cold regions science and engineering series, Part II-B,* US Army Cold Regions Res. and Engr. Lab., Hanover, New Hampshire.

Barkov, I. I., Gordienko, F. G., Korotkevich, E. S. & Kotlyakov, V. M., 1974. First results of the study of an ice core from the borehole at Vostok Station (Antarctica) by the isotope–oxygen method, *Dokl. Akad. Nauk SSSR,* **214,** 1383–1386.

Benfield, A. E., 1951. The temperature in an accumulating snowfield, *Mon. Not. R. astr. Soc. Geophys. Suppl.,* **6,** 139–147.

Dansgaard, W., Johnsen, S. J., Clausen, H. B. & Gundestrup, N., 1973. Stable isotope glaciology, *Meddr Grønland,* **197,** 1–53.

Dansgaard, W. & Johnsen, S. J., 1969. Comment on paper by J. Weertman, 'Comparison between measured and theoretical temperature profiles of the Camp Century, Greenland, borehole', *J. geophys. Res.,* **74,** 1109–1110.

Epstein, S., Sharp, R. P. & Gow, A. J., 1970. Antarctic ice sheet: stable isotope analyses of Byrd station cores and interhemispheric climatic implications, *Science,* **168,** 1570–1572.

Fung, Y. C., 1965. *Foundations of solid mechanics,* Prentice-Hall, Englewood Cliffs.

Glen, J. W., 1958. The flow law of ice: a discussion of the assumptions made in glacier flow theory, their experimental foundations and consequences, *Publ. No. 47,* Int. Assn of Scientific Hydrology, IUGG, Symposium of Chamonix, pp. 171–183.

Johnsen, S. J., 1977. Stable isotope profiles compared with temperature profiles in firn and with historical temperature records, *Publ. No. 118,* Int. Assn of Hydrological Sciences, IUGG, Symposium of Genoble, pp. 388–392.

Johnsen, S. J., Dansgaard, W., Clausen, H. B. & Langway, C. C., Jr, 1972. Oxygen isotope profiles through the Antarctic and Greenland Ice Sheets, *Nature,* **235,** 429–434 and **236,** 249.

Koerner, R. M., 1977. Devon Island ice cap: core stratigraphy and paleoclimate, *Science,* **196,** 15–18.

Paterson, W. S. B., 1976. Vertical strain-rate measurements in an Arctic ice cap and deductions from them, *J. Glaciol.,* **17,** 3–12.

Paterson, W. S. B., Koerner, R. M., Fisher, D., Johnsen, S. J., Clausen, H. B., Dansgaard, W., Bucher, P. & Oeschger, H., 1977. An oxygen-isotope climatic record from the Devon Island Ice Cap, Arctic Canada, *Nature,* **266,** 508–511.

Philberth, K. & Federer, B., 1971. On the temperature profile and the age profile in the central part of cold ice sheets, *J. Glaciol.,* **10,** 3–14.

Prager, W., 1961. *Introduction to the mechanics of continua,* Ginn and Company, New York.

Radok, U., Jenssen, D. & Budd, W., 1970. Steady-state temperature profiles in ice sheets, *Publ. No. 86,* Int. Assn of Scientific Hydrology, IUGG, International Symposium on Antarctic Glaciological Exploration, Hanover, New Hampshire, pp. 151–165.

Robin, G. de Q., 1955. Ice movement and temperature distribution in glaciers and ice sheets, *J. Glaciol.,* **2,** 523–532.

Weertman, J., 1968. Comparison between measured and theoretical temperature profiles of the Camp Century, Greenland, borehole, *J. geophys. Res.,* **73,** 2691–2700.

Weertman, J., 1973. Creep of ice, *Physics and chemistry of ice,* pp. 320–337, eds Whalley, E., Jones, S. J. & Gold, L. W., Royal Society of Canada, Ottawa.

Appendix

The finite-difference scheme we use to approximate (9) is

$$-\lambda\left(1-\frac{\Delta y}{2}\gamma_i\right)T_{i-1}^{N+1}+2\left(\lambda+\frac{\kappa_0}{\kappa_i}\right)T_i^{N+1}-\lambda\left(1+\frac{\Delta y}{2}\gamma_i\right)T_{i+1}^{N+1}$$
$$=+\lambda\left(1-\frac{\Delta y}{2}\gamma_i\right)T_{i-1}^{N}-2\left(\lambda-\frac{\kappa_0}{\kappa_i}\right)T_i^{N}+\lambda\left(1+\frac{\Delta y}{2}\gamma_i\right)T_{i+1}^{N}+F_i^N \qquad \text{(A1)}$$

where the i subscript indicates evaluation at the ith grid point and the N superscript indicates evaluation at the Nth time step. The quantities λ, γ_i and F_i^N in (A1) are defined as

$$\lambda = \kappa_0 \Delta t/(\Delta y)^2$$

$$\gamma_i = \frac{1}{K_i}\left(\frac{dK}{dy}\right)_i - \frac{v_i}{\kappa_i} \tag{A2}$$

and

$$F_i^N = \frac{2\kappa_0 \Delta t f_i^N}{K_i J} = \frac{2\kappa_0 \Delta t}{K_i J}\left[(\sigma_{mn}\dot{\epsilon}_{mn})_i^N + J w_i^N\right]$$

where Δt is the time-step size, Δy the space mesh size and κ_0 the diffusivity at the surface of the ice sheet. A similar equation to (A1) applies in the subglacial bed with the simplification that $\gamma_i = 0$ and $F_i^N = 0$.